Micropeptide ASAP encoded by LINC00467 promotes colorectal cancer progression by directly modulating ATP synthase activity

Supplemental Figures

Figure S1. Characterization of the coding potential of LINC00467.

A The GEO dataset GSE37364 indicates LINC00467 expression levels in CRC tissues (n = 27) and adjacent normal tissues (n = 38). Bounds of box show the 25th and 75th percentiles, and the central lines in the box represent the median value. Whiskers: 10-90 percentile. Outlying value: 8.63, 8.37, 7.87, 6.98, 6.94, 6.70 (N), 9.20, 9.17, 6.99, 6.63 (T). Independent-samples two-sided Student's t-test; $^{**}P < 0.01$.

B and **C** RT-qPCR detection of *LINC00467* expression in cytoplasmic and nuclear fractionations in HCT116 (**B**) and RKO (**C**) cells. *GAPDH* is a mRNA mainly located in the cytoplasm which was used as a cytosolic transcript marker; *XIST* is a lncRNA mainly located in the nucleus which was used as a nuclear transcript marker. Data are presented as mean values ± S.D., $n = 3$ biologically independent experiments.

D Indicated constructs were expressed in HCT116 cells, and the Flag signal was detected by Western blot analysis.

E Diagram of the GFP fusion constructs. The start codon of MutGFP was mutated from ATGGTG to ATTGTT. The start codon of MutORF was mutated from ATG to ATT.

F and **G** The GFP signal in indicated cells was observed in microscope (**F**) and detected by Western blot analysis (**G**). Scale bar, 100 μm.

H The ORF1-Flag fusion protein in Flag-KI HEK293T cells was detected by Western blot analysis.

Data are representative of 3 independent experiments (**D, F-H**).

Figure S2. Sequence, 3D structures, conservative analysis of ASAP peptides.

A The amino acid sequences of the ASAP peptide encoded by the LINC00467 ORF1 of *H. sapiens*. The ATG start codon and TGA stop codon are highlighted in red.

B 3D structures of ASAP peptide were modeled by C-I-TASSER algorithm.

C Multi-species alignment of the ASAP using PRALINE algorithm after *in silico* translation of the conserved homologous ORFs in the indicated species.

Figure S3. The establishment of antibody and cell lines used in the study.

A HCT116 cells were transfected with anti-*LINC00467* siRNAs, and *LINC00467* levels were determined by RT-qPCR. Data are presented as mean values ± S.D. from $n = 3$ biologically independent experiments. One-way ANOVA followed by Tukey test; ***$P < 0.001$.

B HCT116 cells were transfected with anti-*LINC00467* siRNAs, and ASAP levels were detected by Western blot analysis.

C The expression of ASAP peptide in RKO cells was detected by immunofluorescence with prepared anti-ASAP antibody. Scale bar, 10 μm.

D The expression of ASAP peptide in CRC cells was detected using Western blot analysis.

E ASAP-3×Flag construct was transfected into HCT116 and RKO cells. Immune blot using anti-ASAP antibody was performed to detect endogenous ASAP and exogenous Flag-ASAP in the same IB.

F Schematic diagram showing the ASAP KO strategy in CRC cell lines using a CRISPR/Cas9 system.

G The *LINC00467* levels in ASAP KO cells were determined by RT-qPCR. Data are presented as mean values ± S.D. from $n = 3$ biologically independent experiments. Independent-samples two-sided Student's *t*-test.

H The ribosomal *LINC00467* levels in ASAP KO cells were determined by polysome profiling followed by RT-qPCR. Data are presented as mean values ± S.D. from $n = 3$ biologically independent experiments. Independent-samples two-sided Student's *t*-test; ***$P < 0.001$.

I The ASAP levels in ASAP KO cells were determined by Western blot analysis.

J-M The ASAP levels in indicated cells were determined by Western blot analysis.

Data are representative of 3 independent experiments (**B-E, I-M**).

Figure S4. ASAP is localized in mitochondria.

A Line scan of the relative fluorescence intensity of the signal (dotted line in **Figure 2B**) is plotted to show the peak overlapping.

B The immunofluorescence of ASAP (green) and MitoTraker (red) in RKO cells. Nuclei

were stained with DAPI (blue). Scale bar, 10 μm.

C Line scan of the relative fluorescence intensity of the signal (dotted line in **Figure S4B**) is plotted to show the peak overlapping.

D Immunoblot detection of ASAP in the purified mitochondria from RKO cells with the indicated protein markers to confirm the efficiency of the established isolation method for mitochondria (SDHA and TOM20 for mitochondria and Vinculin and α-Tubulin for the cytosol). Cyto, cytosol; Mito, mitochondria.

E Mitochondria were isolated from RKO cells and subjected to proteinase K (PK) digestion at the indicated concentrations at 37 ℃. Mitochondria lysed in RIPA buffer served as a control for the total mitochondrial fraction. Western blots were performed for markers of the OMM (TOM20), IMM (ATP5A), or endogenous ASAP protein.

F Mitochondria were isolated from RKO cells and subjected to PK (10^3 ng/mL) proteolysis in the presence or absence of detergent (1% Triton). Western blot analysis was performed using antibodies for ASAP or for the sub-mitochondrial markers ATP5A and TOM20.

G Line scan of the relative fluorescence intensity of the signal (dotted line in **Figure 2F**) was plotted to show the peak overlapping.

Data are representative of 3 independent experiments (**B, D-F**).

Figure S5. ASAP regulates mitochondrial ATP production.

A-C Relative mitochondrial ATP production was detected. Indicated HCT116 and RKO cells were treated with recording buffer (with 5 mM 2-DG and 5 mM pyruvate) to determine ATP generation under mitochondrial ATP synthesis. Data are presented as mean values ± S.D. from $n = 6$ biologically independent experiments. One-way ANOVA followed by Tukey test; ***$P < 0.001$.

D-G The relative whole cell ATP production of indicated HCT116 and RKO cells was detected. Data are presented as mean values ± S.D. from $n = 6$ biologically independent experiments. One-way ANOVA followed by Tukey test; ***$P < 0.001$.

H-J Oxygen consumption rate (OCR) profile was monitored in indicated HCT116 and RKO cells with a Seahorse XF24 analyzer for 75 min. The metabolic inhibitors were injected sequentially at different time points as indicated. Data are presented as mean values ± S.D., $n = 3$ biologically independent experiments.

Figure S6. ASAP promotes colorectal cancer cell proliferation in vitro.

A and **B** The colony formation assay was performed on wild-type, ASAP, LINC00467 (Lnc467 for short), or Mut-LINC00467 (Mut-Lnc467 for short)-overexpressing HCT116 (**A**) or RKO (**B**) cells. Representative images from each group (left) and statistical analysis (right) are shown. Data are presented as mean values ± S.D. from $n = 3$ biologically independent experiments. One-way ANOVA followed by Tukey test; ***$P < 0.001$.

C and **D** The colony formation assay was performed on wild-type, ASAP KO, LINC00467 (Lnc467 for short), or Mut-LINC00467 (Mut-Lnc467 for short)-restored HCT116 (**C**) or RKO (**D**) cells. Representative images (left) from each group and statistical analysis (right) are shown. Data are presented as mean values ± S.D. from $n = 3$ biologically independent experiments. One-way ANOVA followed by Tukey test; ***$P < 0.001$.

Figure S7. ASAP promotes colorectal cancer cell proliferation in vivo.

A and **B** The weight of tumors from **Figure 3E** (**A**) and **Figure 3G** (**B**). Data are presented as mean values ± S.D. from $n = 5$ tumor per group. One-way ANOVA followed by Tukey test; ***$P < 0.001$.

C Representative IHC staining in randomly selected tumors from **Figure 3E** and **Figure 3G** are shown. Scale bar, 200 μm.

D and **E** The relative intensities of IHC (**Figure S7C**) were quantified in 10 random fields from 5 tumors in each group by ImageJ software (version 1.51). Data are presented as mean values ± S.D. from $n = 5$ tumor samples per group. One-way ANOVA followed by Tukey test; ***$P < 0.001$.

F and **G** The weight of tumors from **Figure 3I** (**F**) and **Figure 3K** (**G**). Data are presented as mean values ± S.D. from $n = 5$ tumor per group. One-way ANOVA followed by Tukey test; ***$P < 0.001$.

Figure S8. The expression and biological behavior of ASAP in normal intestinal epithelial cells.

A Immune blot was performed to detect ASAP levels in indicated cell lines.

B Western blot detection of ASAP in the purified mitochondria from NCM460 cells with the indicated protein markers to confirm the efficiency of the established isolation method

for mitochondria (SDHA and TOM20 for mitochondria and Vinculin and α-Tubulin for the cytosol). Cyto, cytosol; Mito, mitochondria.

C The immunofluorescence of ASAP (green) and MitoTraker (red) in NCM460 cells. Scale bar, 10 μm.

D The CCK-8 assay was used to determine the proliferation rate of indicated cells. Data are presented as mean values ± S.D., $n = 3$ biologically independent experiments. Two-way ANOVA; $***P < 0.001$.

E Mitochondrial ATP production was detected. Indicated NCM460 cells were treated with recording buffer (with 5 mM 2-DG and 5 mM pyruvate) to determine ATP generation under mitochondrial ATP synthesis. Data are presented as mean values ± S.D. from $n = 6$ biologically independent experiments. Independent-samples two-sided Student's *t*-test; $***P < 0.001$.

F The CCK-8 assay was used to determine the proliferation rate of indicated cells. Data are presented as mean values ± S.D., $n = 3$ biologically independent experiments. Two-way ANOVA.

G Mitochondrial ATP production was detected. Indicated NCM460 cells were treated with recording buffer (with 5 mM 2-DG and 5 mM pyruvate) to determine ATP generation under mitochondrial ATP synthesis. Data are presented as mean values ± S.D. from $n = 6$ biologically independent experiments. Independent-samples two-sided Student's *t*-test.

Data are representative of 3 independent experiments (**A-C**).

Figure S9. Identification of interplay between ASAP and candidate proteins.

A-C ATP5B-His (**A**), HADHA-His (**B**), or SLC25A3-His (**C**) were co-overexpressed with SFB-ASAP in HEK293T cells. Co-IP assays were performed to detect the ASAP-ATP5B (**A**), ASAP-HADHA (**B**) and ASAP-SLC25A3 (**C**) interaction.

D Co-IP assays showing the endogenous interaction between ASAP and both ATP5A and ATP5C in NCM460 cells.

E ASAP-His was co-expressed SFB-ATP5A, SFB-ATP5B, SFB-ATP5C, SFB-ATP5D, SFB-ATP5E, respectively. Co-IP assays was performed to detect the interaction between ASAP and ATP synthase F1 domain subunits.

F The protein levels of ATP5A and ATP5C in indicated cells were detected by Western blot analysis.

G and **H** The relative activities of respiratory Complex V (ATP Synthase) were investigated in tumors from **Figure 3E** and **Figure 3G**. Data are presented as mean values ± S.D. from $n = 5$ tumor samples per group. One-way ANOVA followed by Tukey test; ***$P < 0.001$. Data are representative of 3 independent experiments (**A-F**).

Figure S10. Molecular docking indicates key residues of ASAP contribute to interaction between ASAP and ATP synthase.

A Molecular docking analysis of ASAP and ATP synthase (Only one ATP5A and ATP5C are shown).

B Molecular docking shows critical residues contribute to ASAP-ATP5A interaction.

C Molecular docking shows critical residues contribute to ASAP-ATP5C interaction.

D SFB-ATP5A was co-overexpressed with WT or mutant ASAP (D65A) in HEK293T cells. Co-IP assays were performed to detect the ASAP-ATP5A interaction.

E SFB-ATP5C was co-overexpressed with WT or mutant ASAP (K79A) in HEK293T cells. Co-IP assays were performed to detect the ASAP-ATP5C interaction.

F SFB-ATP5A was co-overexpressed with WT or Mut-ASAP (K79A and D65A) in HEK293T cells. Co-IP assays were performed to detect the ASAP-ATP5A interaction.

G SFB-ATP5C was co-overexpressed with WT or Mut-ASAP (K79A and D65A) in HEK293T cells. Co-IP assays were performed to detect the ASAP-ATP5C interaction.

H and **I** Flag-Mut-ASAP constructs were infected in HCT116 (**H**) and RKO (**I**) cells, and Flag signal (green) and markers of the mitochondria (MitoTraker, red) were detected using immunofluorescence staining. Scale bar, 10 μm.

Data are representative of 3 independent experiments (**D-I**).

Figure S11. The interaction between ASAP and ATP synthase is crucial for the function of ASAP.

A and **B** The relative whole cell ATP production of indicated HCT116 (**A**) and RKO (**B**) cells was detected. Data are presented as mean values ± S.D. from $n = 6$ biologically independent experiments. One-way ANOVA followed by Tukey test; ***$P < 0.001$.

C and **D** The relative activities of respiratory Complex V (ATP Synthase) were investigated in indicated HCT116 (**C**) and RKO (**D**) cells. Data are presented as mean values ± S.D., $n = 6$ biologically independent experiments. One-way ANOVA followed by Tukey test;

***$P < 0.001$.

E and **F** Relative mitochondrial ATP production was detected. Wild-type, ASAP KO, ASAP or Mut-ASAP-restored HCT116 (**E**) and RKO (**F**) cells were treated with recording buffer (with 5 mM 2-DG and 5 mM pyruvate) to determine ATP generation under mitochondrial ATP synthesis. Data are presented as mean values ± S.D. from $n = 6$ biologically independent experiments. One-way ANOVA followed by Tukey test; ***$P < 0.001$.

G and **H** The relative whole cell ATP production of indicated HCT116 (**G**) and RKO (**H**) cells was detected. Data are presented as mean values ± S.D. from $n = 6$ biologically independent experiments. One-way ANOVA followed by Tukey test; ***$P < 0.001$.

I and **J** The CCK-8 assay was used to determine the proliferation rate of indicated HCT116 (**I**) and RKO (**J**) cells. Data are presented as mean values ± S.D., $n = 3$ biologically independent experiments. Two-way ANOVA analysis; ***$P < 0.001$.

K The weight of tumors from **Figure 7G**. Data are presented as mean values ± S.D. from $n = 5$ tumor samples per group. One-way ANOVA followed by Tukey test; ***$P < 0.001$.

L The relative activities of respiratory Complex V (ATP Synthase) were investigated in tumors from **Figure 7G**. Data are presented as mean values ± S.D. from $n = 5$ tumor samples per group. One-way ANOVA followed by Tukey test; ***$P < 0.001$.

Figure S12. ASAP regulates CRC growth through mitochondrial ATP synthase

A The weight of tumors from **Figure 7I**. Data are presented as mean values ± S.D. from $n = 5$ tumor per group. One-way ANOVA followed by Tukey test; *$P < 0.05$, ***$P < 0.001$.

B Xenograft mouse model using EV control or ASAP overexpressing RKO cells with or without the treatment of Oligomycin. In vivo generated tumors are shown.

C Analyses of tumor growth and volume in xenograft mouse model of **Figure S12B** are shown. Data are presented as mean values ± S.D. from $n = 5$ mice per group. Two-way ANOVA analysis; *$P < 0.05$, ***$P < 0.001$.

D The weight of tumors from **Figure S12B**. Data are presented as mean values ± S.D. from $n = 5$ tumors per group. One-way ANOVA followed by Tukey test; *$P < 0.05$, ***$P < 0.001$.

E and **F** The colony formation assay was performed on wild-type (WT), ASAP Knockout (KO) RKO cells. KO cells were supplied with additional 3 mM ADP or 3 mM ATP. Representative images from each group (**E**) and statistical analysis (**F**) are shown. Data are

presented as mean values ± S.D. from $n = 3$ biologically independent experiments. One-way ANOVA followed by Tukey test; ***$P < 0.001$.

Figure S13. Targeting ASAP suppresses the growth of patient derived xenografts.

A and **B** Analyses of tumor growth and volume in PDX models. Two-way ANOVA analysis; ***$P < 0.001$.

C and **D** The ASAP levels in tumors from PDX mice were determined by Western blot analysis.

E and **F** The relative activities of respiratory Complex V (ATP Synthase) were investigated in tumors from PDX model. Data are presented as mean values ± S.D. from $n = 5$ tumor samples per group. Independent-samples two-sided Student's *t*-test; ***$P < 0.001$.

Data are representative of 3 independent experiments (**C** and **D**).

Figure S14. The expression of ASAP, ATP5A and ATP5C in colorectal tissues.

A Quantification of ATP5A protein expression by scoring Immunohistochemistry staining in CRC of Cohort 2 ($n = 92$). Bounds of box show the 25th and 75th percentiles, and the central lines in the box represent the median value. Whiskers: 5-95 percentile. Outlying value: 12, 12, 12 (Normal). Paired-samples two-sided Student's *t*-test; ***$P < 0.001$.

B Quantification of ATP5C protein expression by scoring Immunohistochemistry staining in CRC of Cohort 2 ($n = 92$). Bounds of box show the 25th and 75th percentiles, and the central lines in the box represent the median value. Whiskers: 5-95 percentile. Outlying value: 16, 12, 12, 12 (Normal) and 16, 16, 16 (Tumor). Paired-samples two-sided Student's *t*-test; ***$P < 0.001$.

C Representative images of ASAP staining on normal colonic tissues. Scale bar, 100 μm.

Data are representative of 3 independent experiments (**C**).

Figure S15. Recombinant proteins used in the study.

A Coomassie staining of bacterial purified MBP-ATP5A-His protein and MBP-ATP5C-His protein.

B Coomassie staining of bacterial purified ASAP-His protein and GST-ASAP protein.

C Coomassie staining of bacterial purified GST-ATP5A protein and GST-ATP5C protein.

Data are representative of 3 independent experiments (**A-C**).

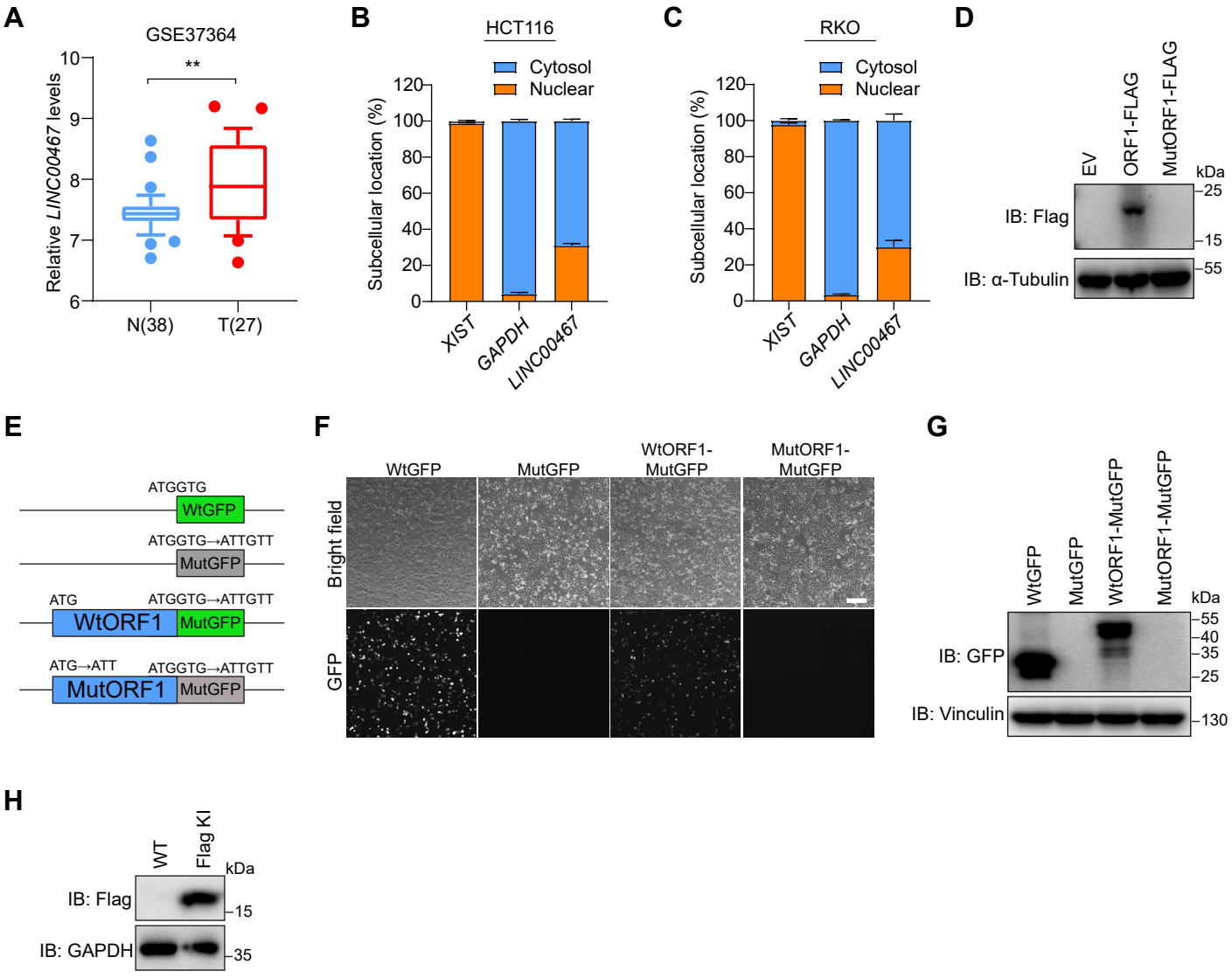
A
GSE37364
**
Relative LINC00467 levels
10
9
8
7
6
N(38)
T(27)
B
HCT116
Cytosol
Nuclear
Subcellular location (%)
120
100
80
60
40
20
0
XIST
GAPDH
LINC00467
C
RKO
Cytosol
Nuclear
Subcellular location (%)
XIST
GAPDH
LINC00467
D
EV
ORF1-FLAG
MutORF1-FLAG
kDa
IB: Flag
25
15
IB: α-Tubulin
55
E
ATGGTG
WtGFP
ATGGTG→ATTGTT
MutGFP
ATG
ATGGTG→ATTGTT
WtORF1
MutGFP
ATG→ATT
ATGGTG→ATTGTT
MutORF1
MutGFP
F
WtGFP
MutGFP
WtORF1-MutGFP
MutORF1-MutGFP
Bright field
GFP
G
WtGFP
MutGFP
WtORF1-MutGFP
MutORF1-MutGFP
kDa
IB: GFP
55
40
35
25
IB: Vinculin
130
H
WT
Flag KI
kDa
IB: Flag
15
IB: GAPDH
35

Figure S1

A

```
ATG GAT AAG AAG TCC ACT CAC AGA AAT CCT GAA GAT GCC AGG GCT GGC AAA TAT
 M   D   K   K   S   T   H   R   N   P   E   D   A   R   A   G   K   Y
GAA GGT AAA CAC AAA CGA AAG AAA AGA AGA AAG CAA AAC CAA AAC CAG CAC CGA
 E   G   K   H   K   R   K   K   R   R   K   Q   N   Q   N   Q   H   R
TCC CGA CAT AGA TCA GTG ACG TCT TTT TCT TCA GAT GAT CCT ATG TTT CCT TCT TCC
 S   R   H   R   S   V   T   S   F   S   S   D   D   P   M   F   P   S   S
TCA TCA TCG TCT TCA GGA AGC CAG ACA GAT TCA AGT ATT GAA GAT GCT GCC AAG
 S   S   S   S   S   G   S   Q   T   D   S   S   I   E   D   A   A   K
GGA AAA ATT AAG AAG AAG AGA AGA GAG AAA ACA AAT AAA TGG GAA AAA AGA AAG
 G   K   I   K   K   K   R   R   E   K   T   N   K   W   E   K   R   K
GAC AAA ATA TGA
 D   K   I
```

B

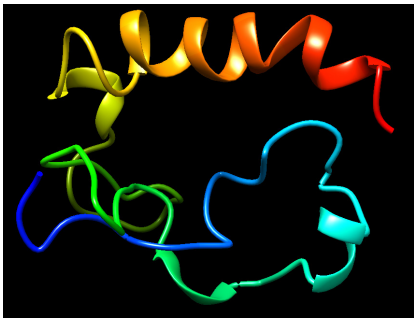

C

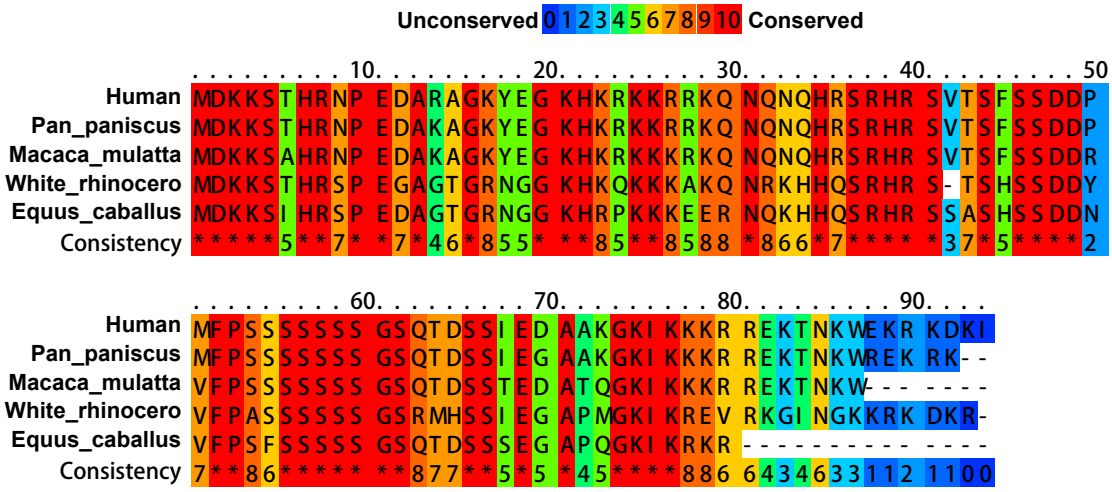

Figure S2

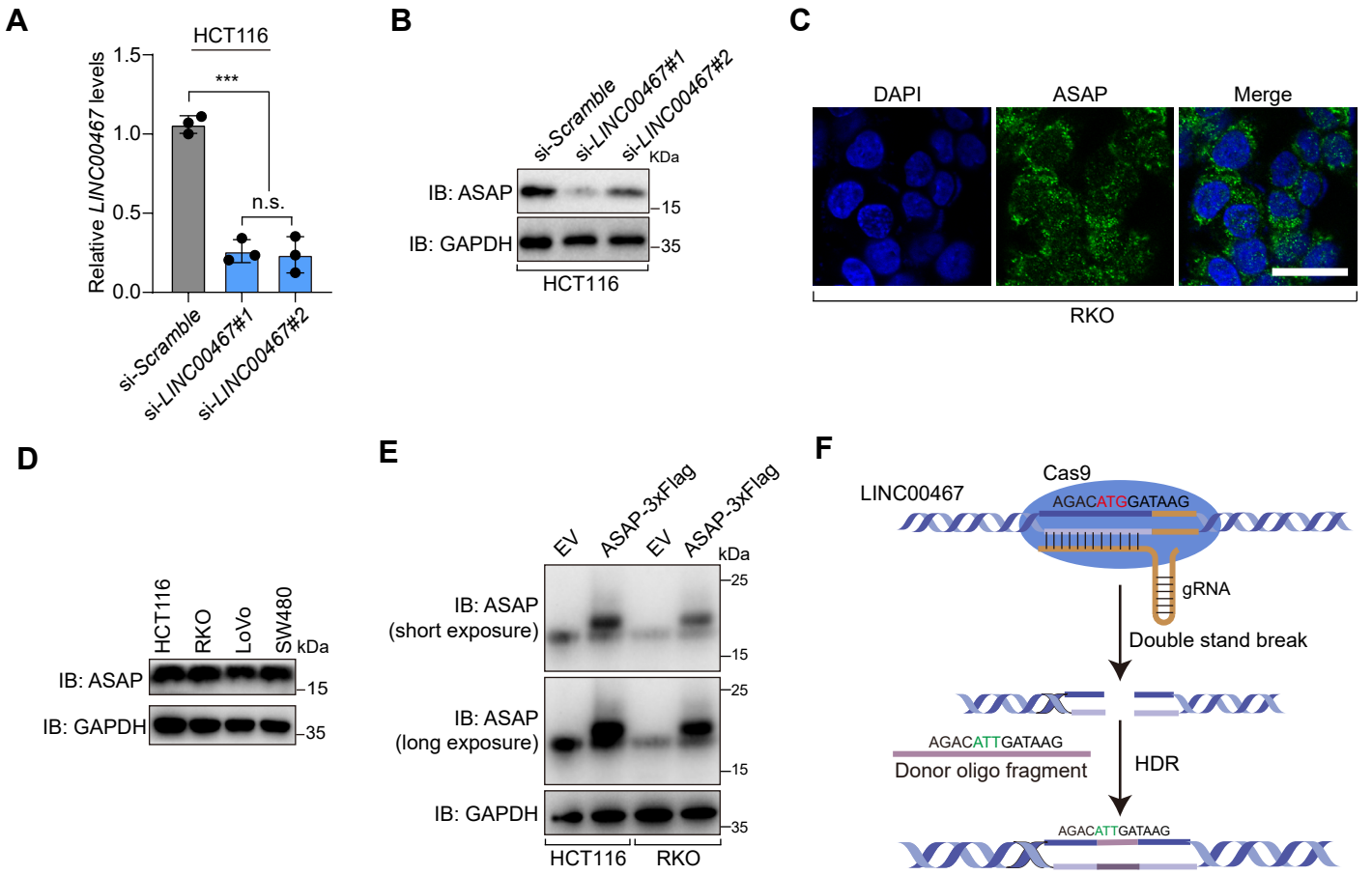
A
HCT116
Relative LINC00467 levels
***
n.s.
si-Scramble
si-LINC00467#1
si-LINC00467#2
B
si-Scramble
si-LINC00467#1
si-LINC00467#2
KDa
IB: ASAP
IB: GAPDH
HCT116
C
DAPI
ASAP
Merge
RKO
D
HCT116
RKO
LoVo
SW480
kDa
IB: ASAP
IB: GAPDH
E
EV
ASAP-3xFlag
EV
ASAP-3xFlag
kDa
IB: ASAP
(short exposure)
IB: ASAP
(long exposure)
IB: GAPDH
HCT116
RKO
F
LINC00467
Cas9
AGACATGGATAAG
gRNA
Double stand break
AGACATTGATAAG
Donor oligo fragment
HDR
AGACATTGATAAG
G
HCT116
RKO
Relative LINC00467 levels in the whole cell
n.s.
WT
ASAP KO
H
HCT116
RKO
Relative Ribosomal LINC00467 levels
***
I
WT
ASAP KO
WT
ASAP KO
KDa
IB: ASAP
IB: GAPDH
HCT116
RKO
J
EV
ASAP
Lnc467
Mut-Lnc467
KDa
IB: ASAP
IB: GAPDH
HCT116
K
ASAP KO
WT
EV
Lnc467
Mut-Lnc467
KDa
IB: ASAP
IB: GAPDH
HCT116
L
EV
ASAP
Lnc467
Mut-Lnc467
KDa
IB: ASAP
IB: GAPDH
RKO
M
ASAP KO
WT
EV
Lnc467
Mut-Lnc467
KDa
IB: ASAP
IB: GAPDH
RKO

Figure S3

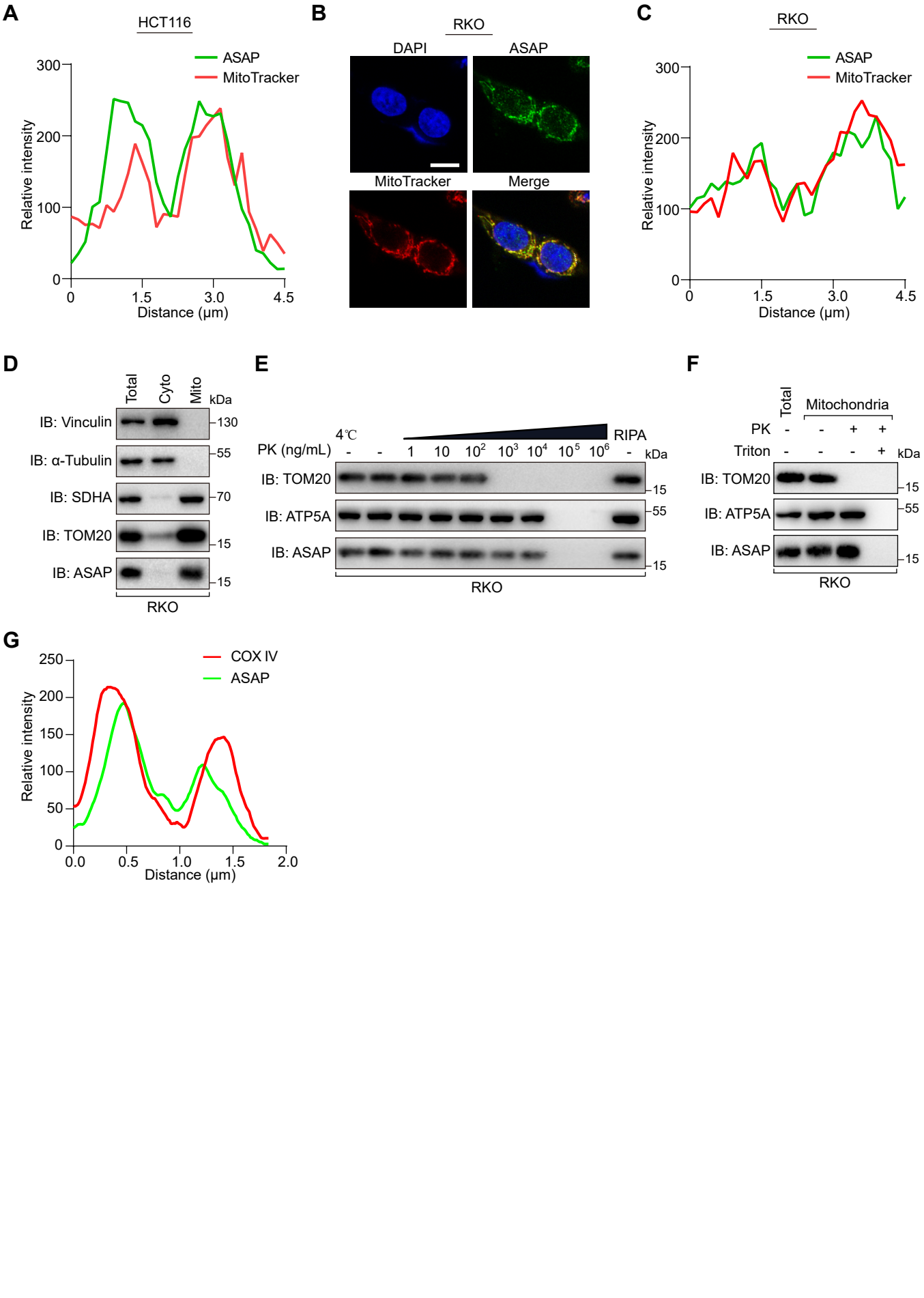
A
HCT116
ASAP
MitoTracker
Relative intensity
Distance (μm)
B
RKO
DAPI
ASAP
MitoTracker
Merge
C
RKO
ASAP
MitoTracker
Relative intensity
Distance (μm)
D
Total
Cyto
Mito
kDa
IB: Vinculin
IB: α-Tubulin
IB: SDHA
IB: TOM20
IB: ASAP
RKO
E
4℃
RIPA
PK (ng/mL)
kDa
IB: TOM20
IB: ATP5A
IB: ASAP
RKO
F
Total
Mitochondria
PK
Triton
kDa
IB: TOM20
IB: ATP5A
IB: ASAP
RKO
G
COX IV
ASAP
Relative intensity
Distance (μm)

Figure S4

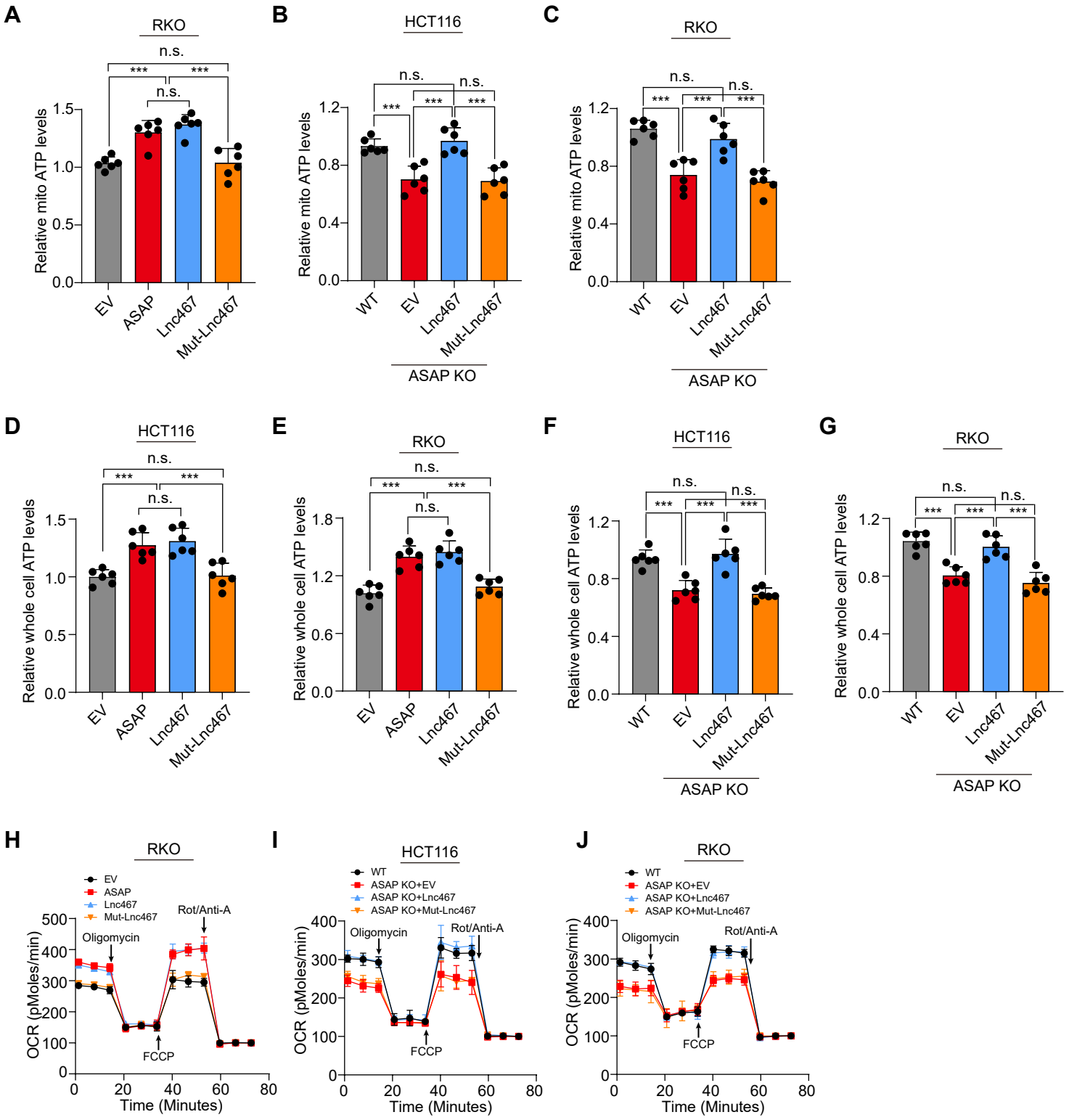
A
RKO
Relative mito ATP levels
EV
ASAP
Lnc467
Mut-Lnc467
B
HCT116
WT
ASAP KO
C
RKO
D
HCT116
Relative whole cell ATP levels
E
RKO
F
HCT116
G
RKO
H
RKO
OCR (pMoles/min)
Time (Minutes)
Oligomycin
FCCP
Rot/Anti-A
I
HCT116
J
RKO
ASAP KO+EV
ASAP KO+Lnc467
ASAP KO+Mut-Lnc467

Figure S5

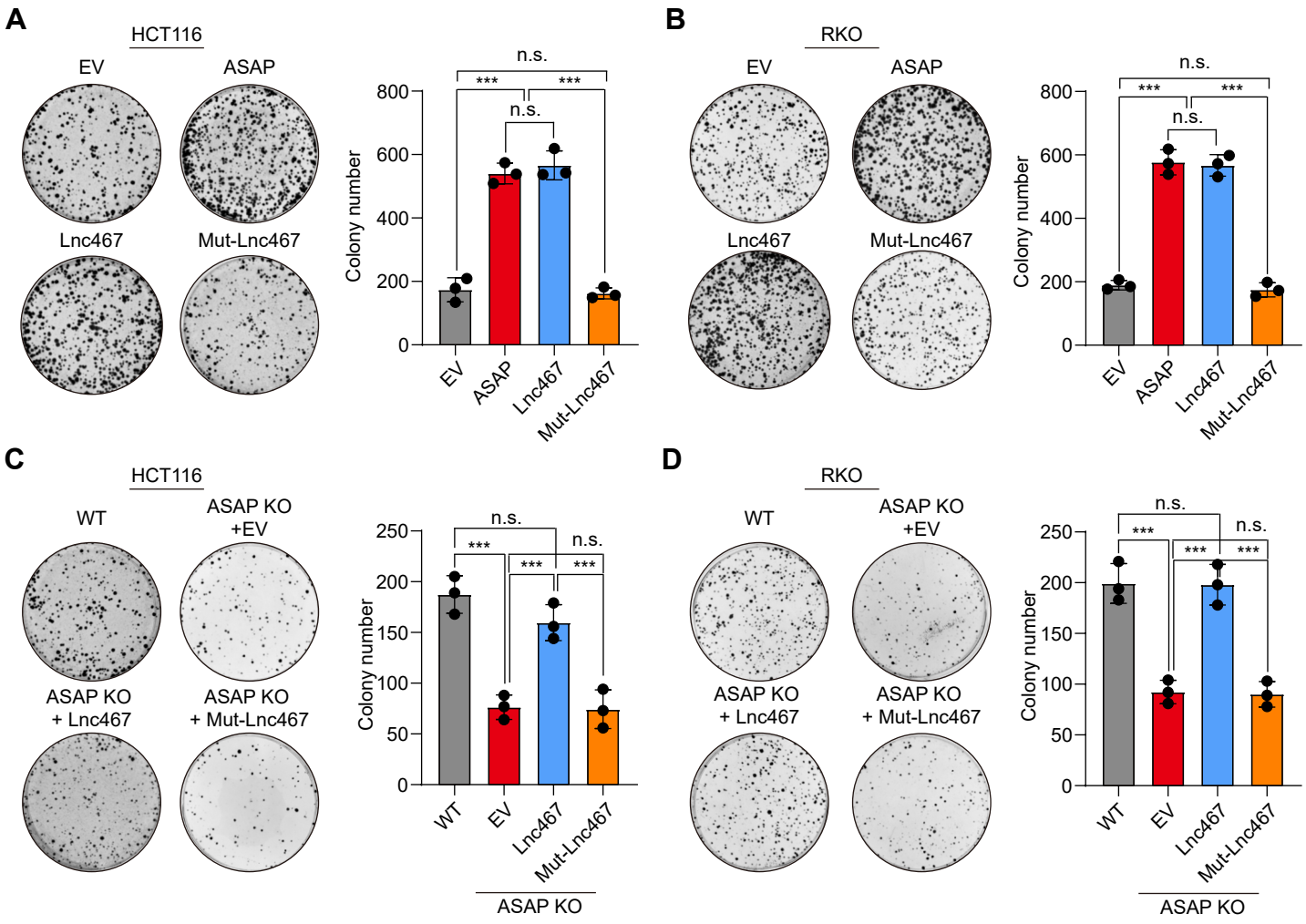
A
HCT116
EV
ASAP
Lnc467
Mut-Lnc467
Colony number
n.s.
***
***
n.s.
800
600
400
200
0
EV
ASAP
Lnc467
Mut-Lnc467
B
RKO
EV
ASAP
Lnc467
Mut-Lnc467
Colony number
n.s.
***
***
n.s.
800
600
400
200
0
EV
ASAP
Lnc467
Mut-Lnc467
C
HCT116
WT
ASAP KO +EV
ASAP KO + Lnc467
ASAP KO + Mut-Lnc467
Colony number
n.s.
***
***
n.s.
***
250
200
150
100
50
0
WT
EV
Lnc467
Mut-Lnc467
ASAP KO
D
RKO
WT
ASAP KO +EV
ASAP KO + Lnc467
ASAP KO + Mut-Lnc467
Colony number
n.s.
***
***
n.s.
***
250
200
150
100
50
0
WT
EV
Lnc467
Mut-Lnc467
ASAP KO

Figure S6

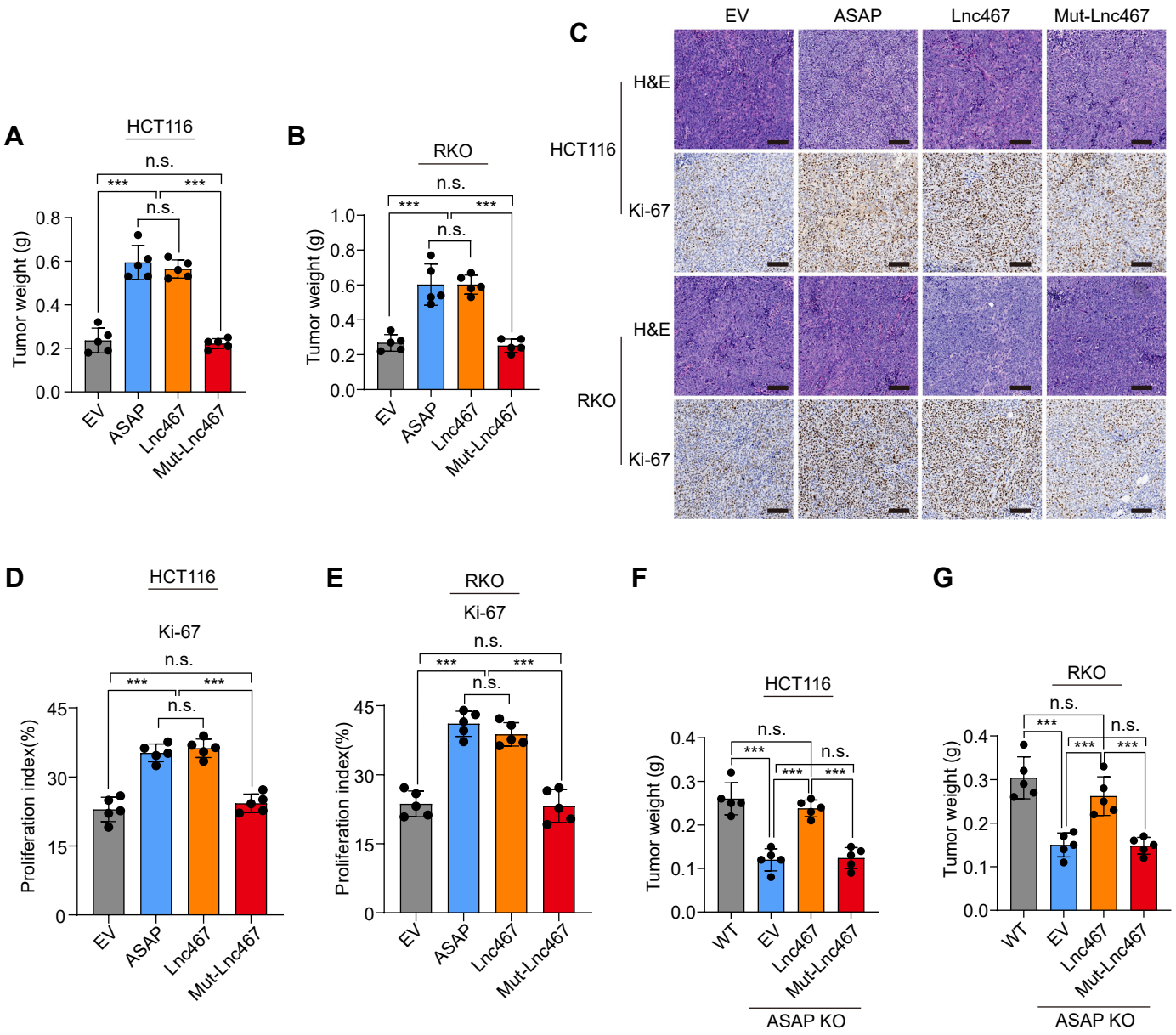
A
HCT116
Tumor weight (g)
n.s.
***
***
n.s.
EV
ASAP
Lnc467
Mut-Lnc467
B
RKO
Tumor weight (g)
C
EV
ASAP
Lnc467
Mut-Lnc467
H&E
HCT116
Ki-67
H&E
RKO
Ki-67
D
HCT116
Ki-67
Proliferation index(%)
E
RKO
Ki-67
Proliferation index(%)
F
HCT116
Tumor weight (g)
WT
ASAP KO
G
RKO
Tumor weight (g)
ASAP KO

Figure S7

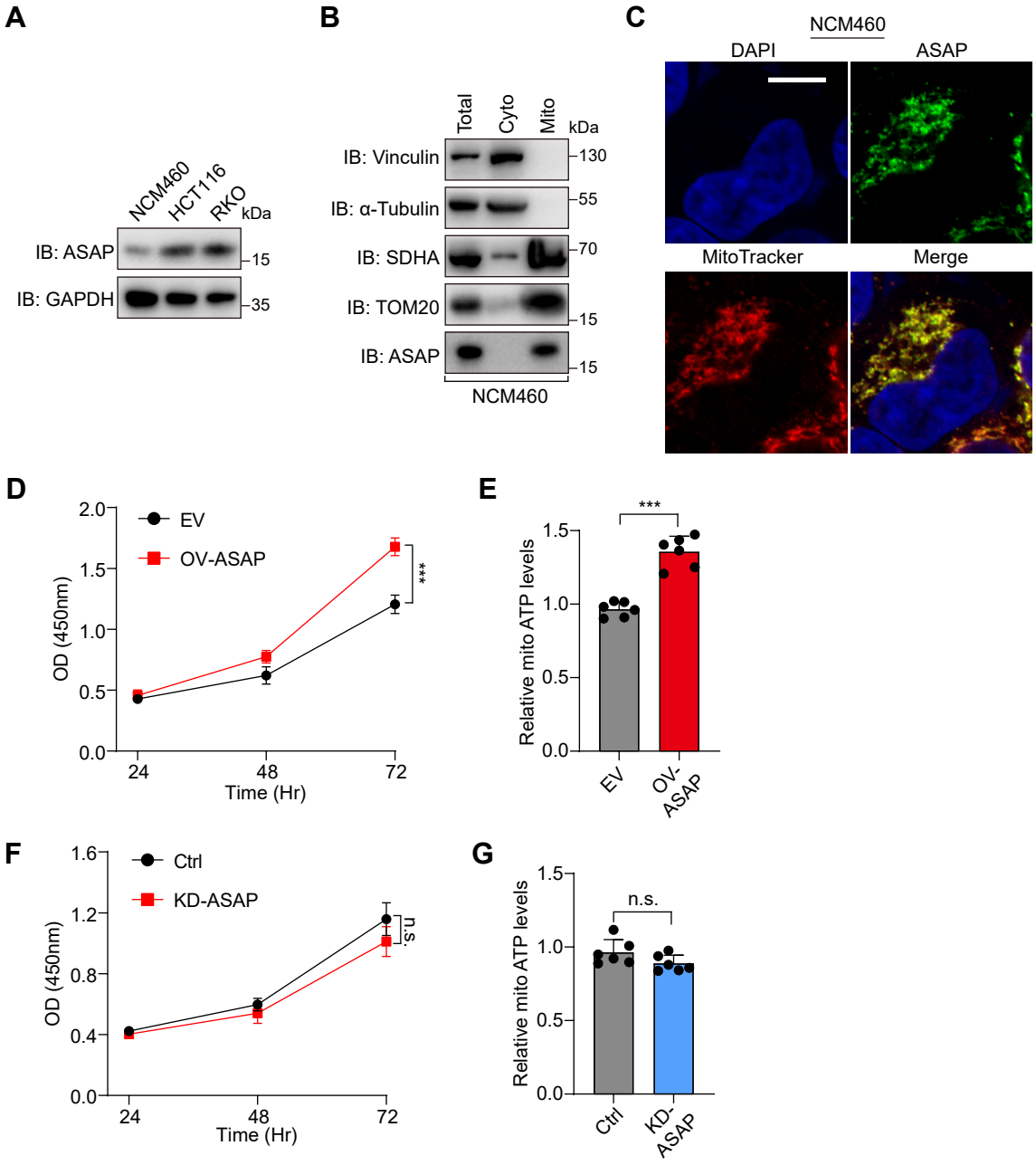
A
NCM460
HCT116
RKO
kDa
IB: ASAP
15
IB: GAPDH
35
B
Total
Cyto
Mito
kDa
IB: Vinculin
130
IB: α-Tubulin
55
IB: SDHA
70
IB: TOM20
15
IB: ASAP
15
NCM460
C
NCM460
DAPI
ASAP
MitoTracker
Merge
D
EV
OV-ASAP
OD (450nm)
2.0
1.5
1.0
0.5
0.0
24
48
72
Time (Hr)
***
E
***
Relative mito ATP levels
1.5
1.0
0.5
0.0
EV
OV-ASAP
F
Ctrl
KD-ASAP
OD (450nm)
1.6
1.2
0.8
0.4
0.0
24
48
72
Time (Hr)
n.s.
G
n.s.
Relative mito ATP levels
1.5
1.0
0.5
0.0
Ctrl
KD-ASAP

Figure S8

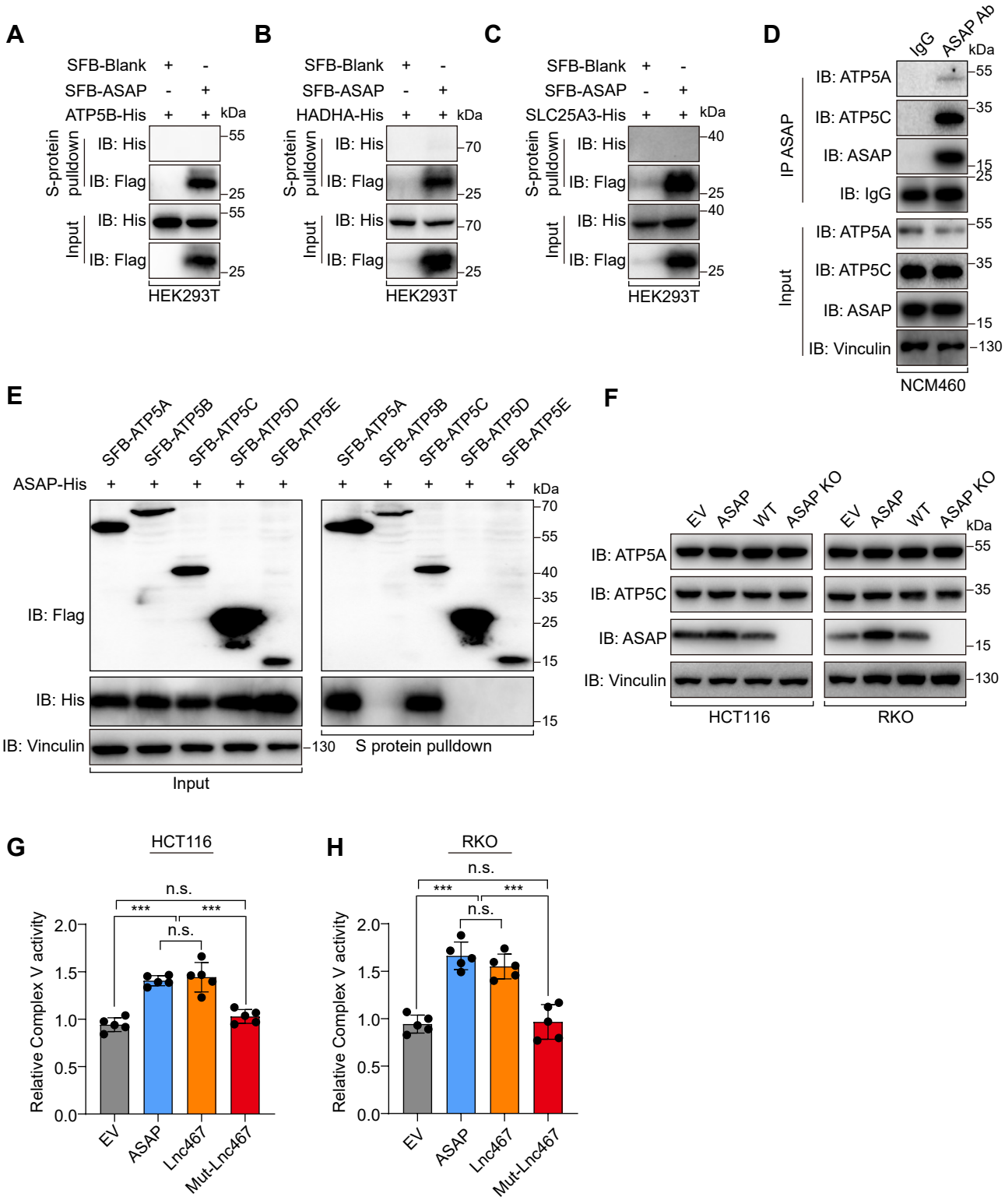
A
SFB-Blank + -
SFB-ASAP - +
ATP5B-His + + kDa
S-protein pulldown
IB: His
IB: Flag
Input
IB: His
IB: Flag
55
25
55
25
HEK293T
B
SFB-Blank + -
SFB-ASAP - +
HADHA-His + + kDa
S-protein pulldown
IB: His
IB: Flag
Input
IB: His
IB: Flag
70
25
70
25
HEK293T
C
SFB-Blank + -
SFB-ASAP - +
SLC25A3-His + + kDa
S-protein pulldown
IB: His
IB: Flag
Input
IB: His
IB: Flag
40
25
40
25
HEK293T
D
IgG
ASAP Ab
kDa
IP ASAP
IB: ATP5A
IB: ATP5C
IB: ASAP
IB: IgG
Input
IB: ATP5A
IB: ATP5C
IB: ASAP
IB: Vinculin
55
35
15
25
55
35
15
130
NCM460
E
SFB-ATP5A
SFB-ATP5B
SFB-ATP5C
SFB-ATP5D
SFB-ATP5E
ASAP-His + + + + +
kDa
IB: Flag
IB: His
IB: Vinculin
70
55
40
35
25
15
130
Input
S protein pulldown
F
EV
ASAP
WT
ASAP KO
kDa
IB: ATP5A
IB: ATP5C
IB: ASAP
IB: Vinculin
55
35
15
130
HCT116
RKO
G
HCT116
Relative Complex V activity
n.s.
***
***
n.s.
2.0
1.5
1.0
0.5
0.0
EV
ASAP
Lnc467
Mut-Lnc467
H
RKO
Relative Complex V activity
n.s.
***
***
n.s.
2.0
1.5
1.0
0.5
0.0
EV
ASAP
Lnc467
Mut-Lnc467

Figure S9

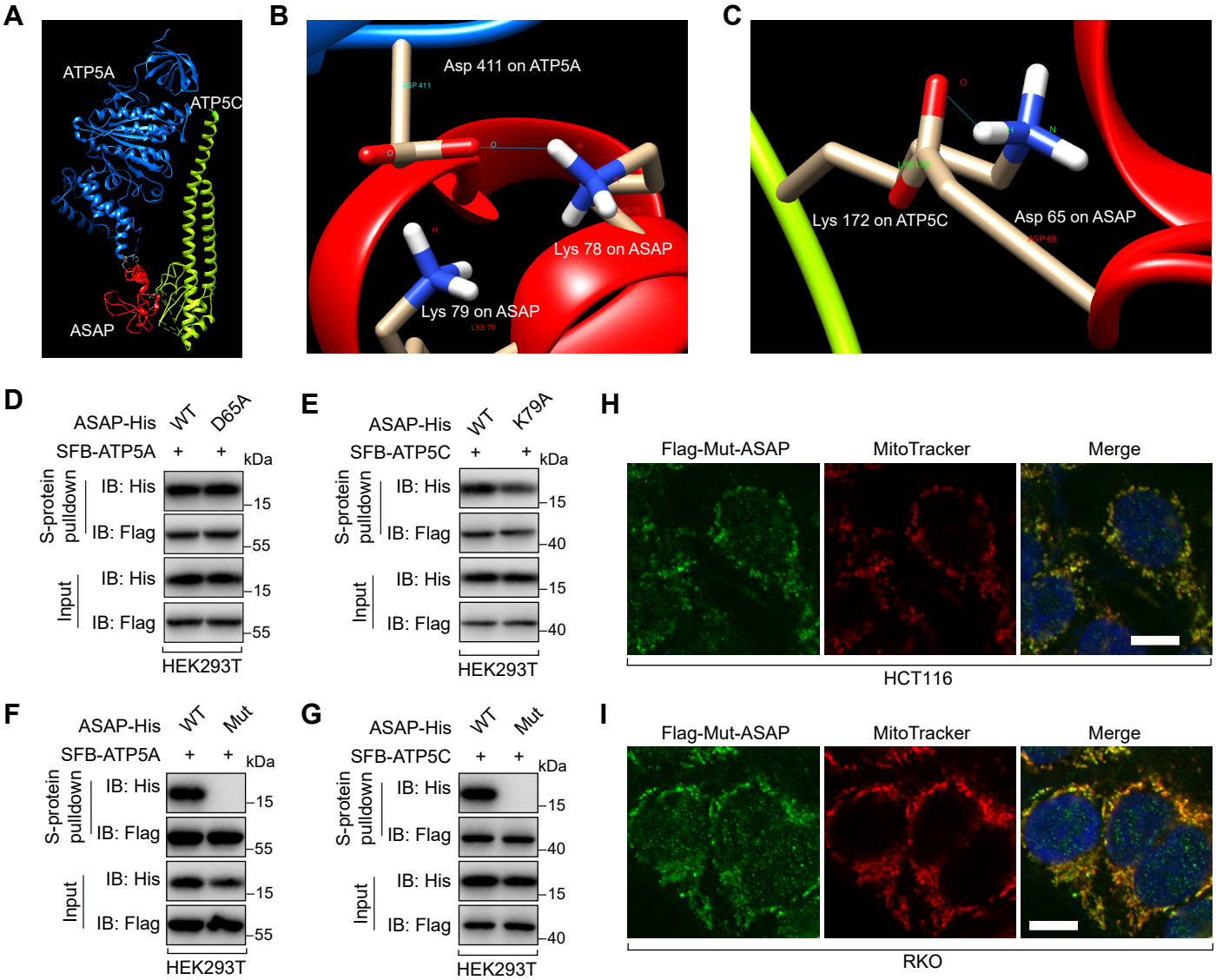
A
ATP5A
ATP5C
ASAP
B
Asp 411 on ATP5A
Lys 78 on ASAP
Lys 79 on ASAP
C
Lys 172 on ATP5C
Asp 65 on ASAP
D
ASAP-His WT D65A
SFB-ATP5A + +
kDa
S-protein pulldown
IB: His
IB: Flag
Input
IB: His
IB: Flag
15
55
15
55
HEK293T
E
ASAP-His WT K79A
SFB-ATP5C + +
kDa
S-protein pulldown
IB: His
IB: Flag
Input
IB: His
IB: Flag
15
40
15
40
HEK293T
H
Flag-Mut-ASAP
MitoTracker
Merge
HCT116
F
ASAP-His WT Mut
SFB-ATP5A + +
kDa
S-protein pulldown
IB: His
IB: Flag
Input
IB: His
IB: Flag
15
55
15
55
HEK293T
G
ASAP-His WT Mut
SFB-ATP5C + +
kDa
S-protein pulldown
IB: His
IB: Flag
Input
IB: His
IB: Flag
15
40
15
40
HEK293T
I
Flag-Mut-ASAP
MitoTracker
Merge
RKO

Figure S10

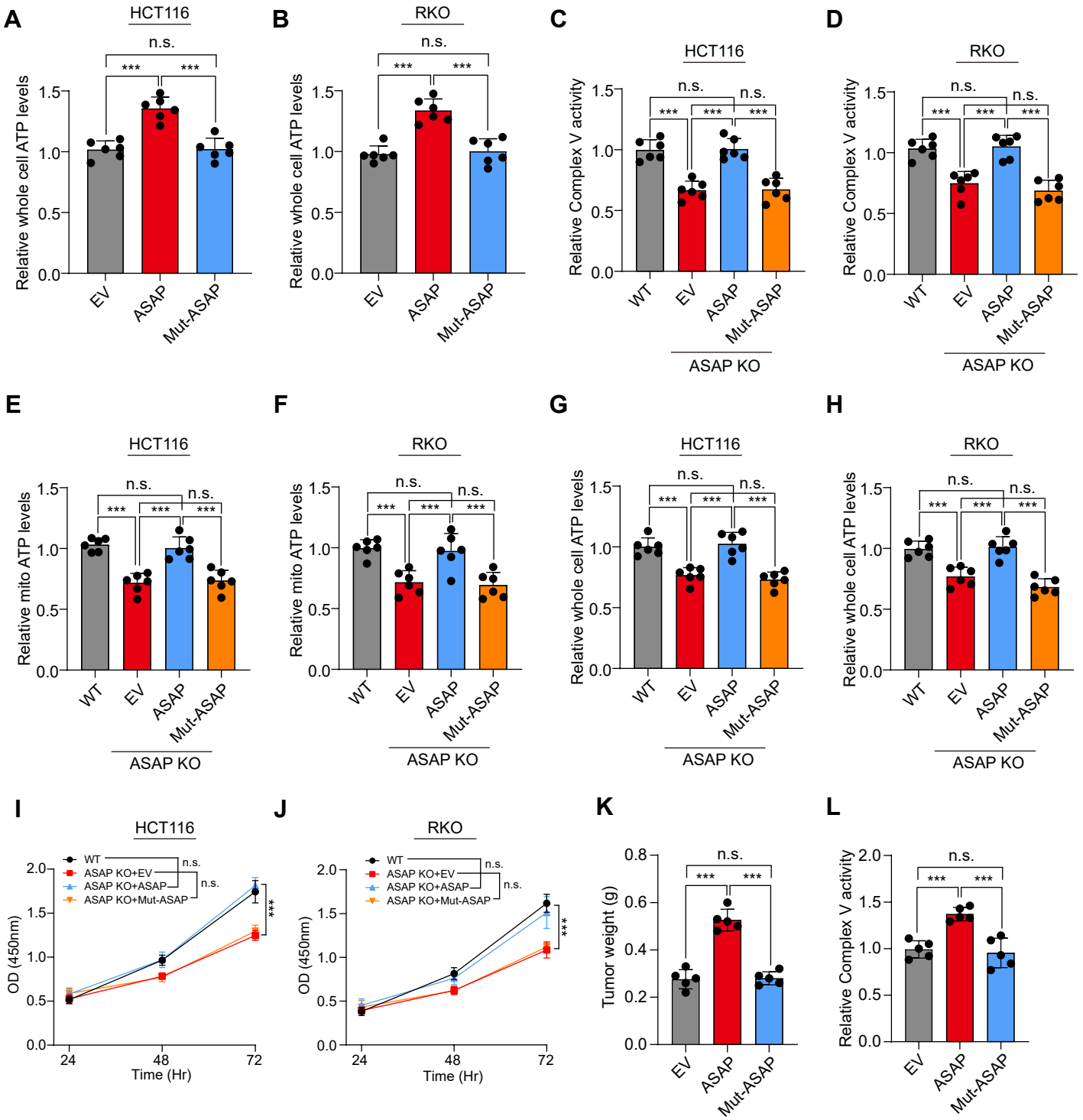
A
HCT116
n.s.
***
***
Relative whole cell ATP levels
1.5
1.0
0.5
0.0
EV
ASAP
Mut-ASAP
B
RKO
n.s.
***
***
Relative whole cell ATP levels
1.5
1.0
0.5
0.0
EV
ASAP
Mut-ASAP
C
HCT116
n.s.
n.s.
***
***
***
Relative Complex V activity
1.5
1.0
0.5
0.0
WT
EV
ASAP
Mut-ASAP
ASAP KO
D
RKO
n.s.
n.s.
***
***
***
Relative Complex V activity
1.5
1.0
0.5
0.0
WT
EV
ASAP
Mut-ASAP
ASAP KO
E
HCT116
n.s.
n.s.
***
***
***
Relative mito ATP levels
1.5
1.0
0.5
0.0
WT
EV
ASAP
Mut-ASAP
ASAP KO
F
RKO
n.s.
n.s.
***
***
***
Relative mito ATP levels
1.5
1.0
0.5
0.0
WT
EV
ASAP
Mut-ASAP
ASAP KO
G
HCT116
n.s.
n.s.
***
***
***
Relative whole cell ATP levels
1.5
1.0
0.5
0.0
WT
EV
ASAP
Mut-ASAP
ASAP KO
H
RKO
n.s.
n.s.
***
***
***
Relative whole cell ATP levels
1.5
1.0
0.5
0.0
WT
EV
ASAP
Mut-ASAP
ASAP KO
I
HCT116
WT
ASAP KO+EV
ASAP KO+ASAP
ASAP KO+Mut-ASAP
n.s.
n.s.
***
OD (450nm)
2.0
1.5
1.0
0.5
0.0
24
48
72
Time (Hr)
J
RKO
WT
ASAP KO+EV
ASAP KO+ASAP
ASAP KO+Mut-ASAP
n.s.
n.s.
***
OD (450nm)
2.0
1.5
1.0
0.5
0.0
24
48
72
Time (Hr)
K
n.s.
***
***
Tumor weight (g)
0.8
0.6
0.4
0.2
0.0
EV
ASAP
Mut-ASAP
L
n.s.
***
***
Relative Complex V activity
2.0
1.5
1.0
0.5
0.0
EV
ASAP
Mut-ASAP

Figure S11

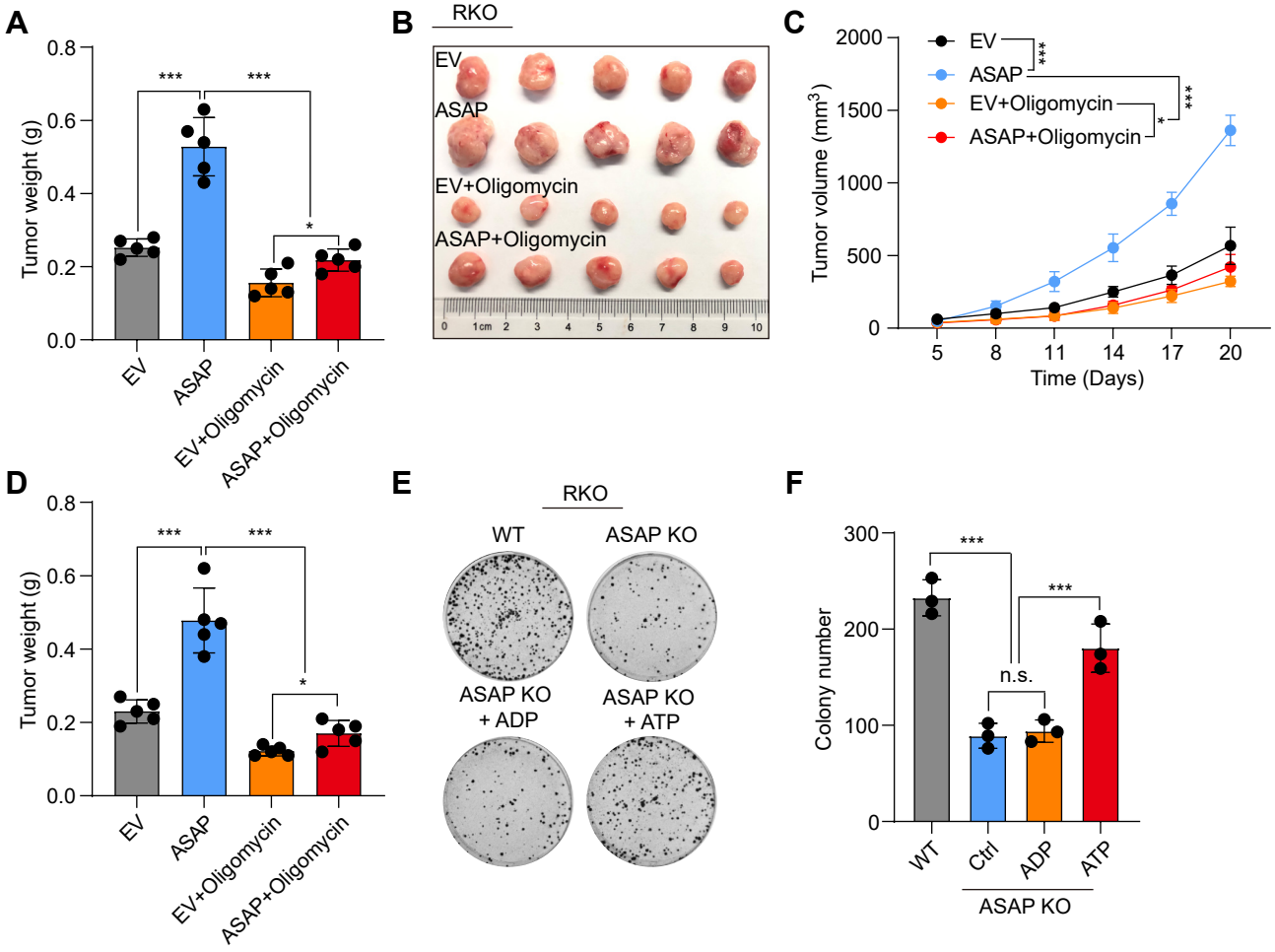
A
Tumor weight (g)
0.8
0.6
0.4
0.2
0.0
***
***
*
EV
ASAP
EV+Oligomycin
ASAP+Oligomycin
B
RKO
EV
ASAP
EV+Oligomycin
ASAP+Oligomycin
C
Tumor volume (mm3)
2000
1500
1000
500
0
EV
ASAP
EV+Oligomycin
ASAP+Oligomycin
***
***
*
5
8
11
14
17
20
Time (Days)
D
Tumor weight (g)
0.8
0.6
0.4
0.2
0.0
***
***
*
EV
ASAP
EV+Oligomycin
ASAP+Oligomycin
E
RKO
WT
ASAP KO
ASAP KO
+ ADP
ASAP KO
+ ATP
F
Colony number
300
200
100
0
***
***
n.s.
WT
Ctrl
ADP
ATP
ASAP KO

Figure S12

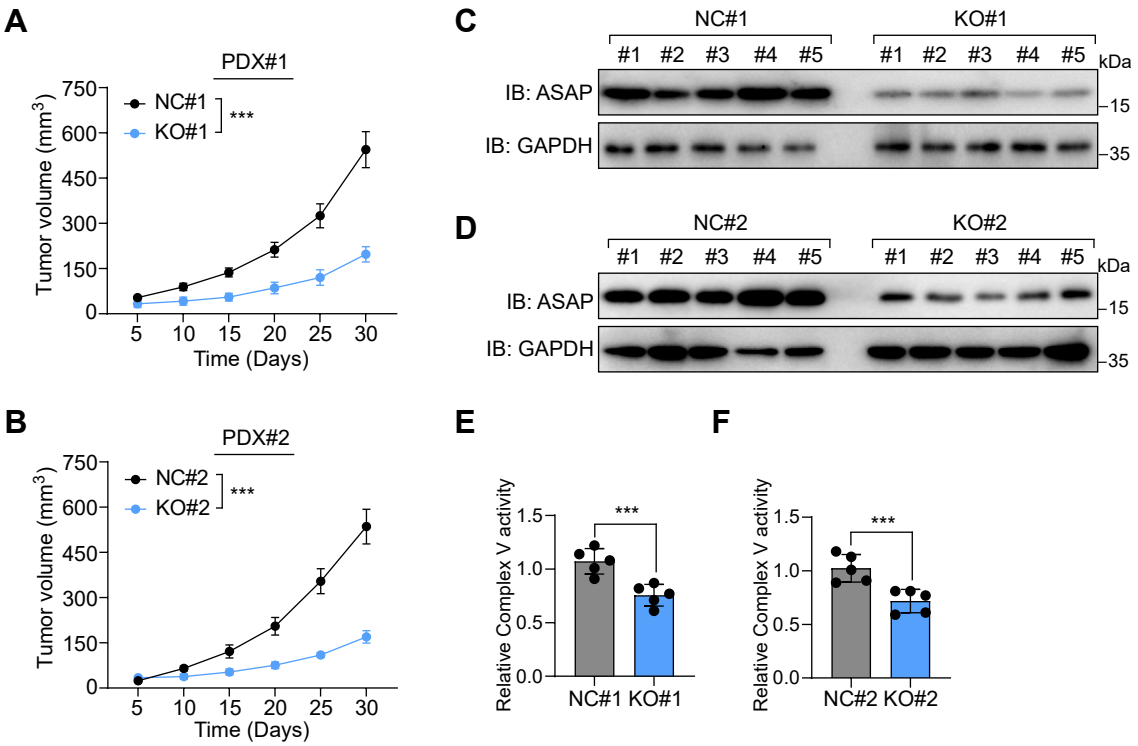
A
PDX#1
NC#1
KO#1
***
Tumor volume (mm3)
Time (Days)
B
PDX#2
NC#2
KO#2
***
Tumor volume (mm3)
Time (Days)
C
NC#1
KO#1
#1 #2 #3 #4 #5
kDa
IB: ASAP
IB: GAPDH
15
35
D
NC#2
KO#2
#1 #2 #3 #4 #5
kDa
IB: ASAP
IB: GAPDH
15
35
E
Relative Complex V activity
***
NC#1 KO#1
F
Relative Complex V activity
***
NC#2 KO#2

Figure S13

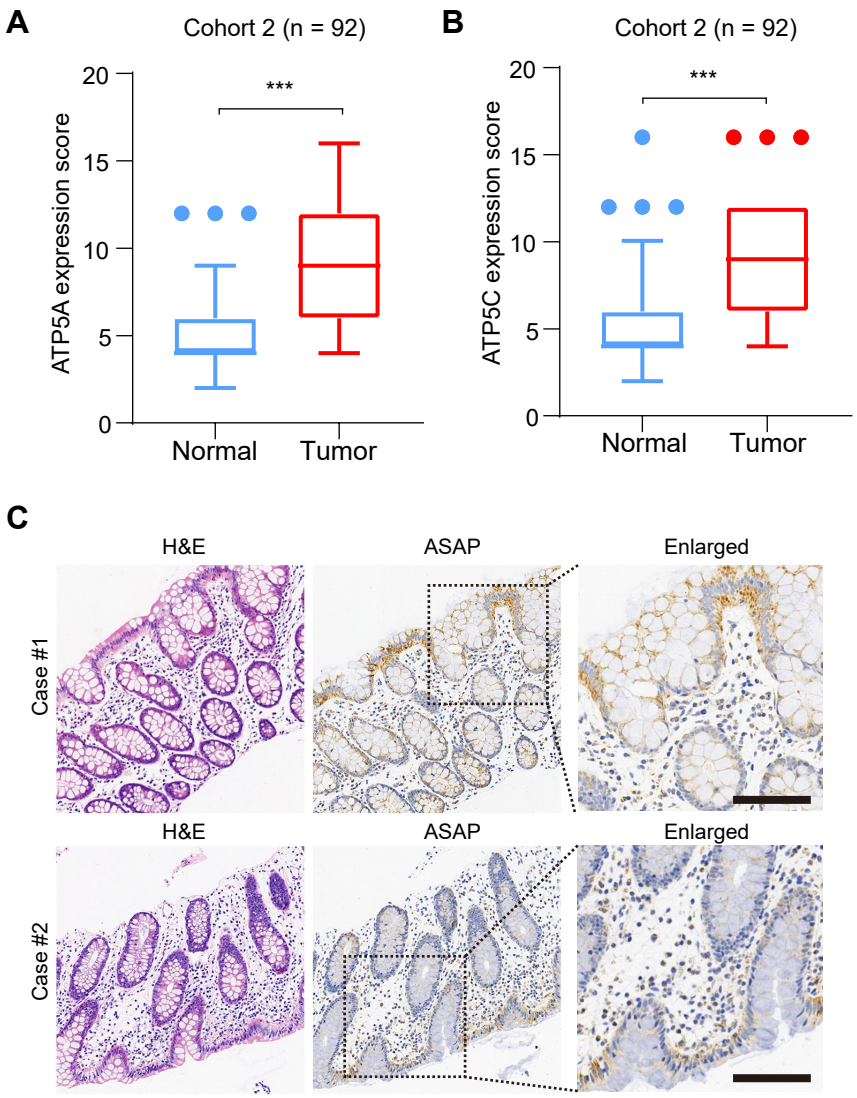
A
Cohort 2 (n = 92)
***
ATP5A expression score
20
15
10
5
0
Normal
Tumor
B
Cohort 2 (n = 92)
***
ATP5C expression score
20
15
10
5
0
Normal
Tumor
C
H&E
ASAP
Enlarged
Case #1
H&E
ASAP
Enlarged
Case #2

Figure S14

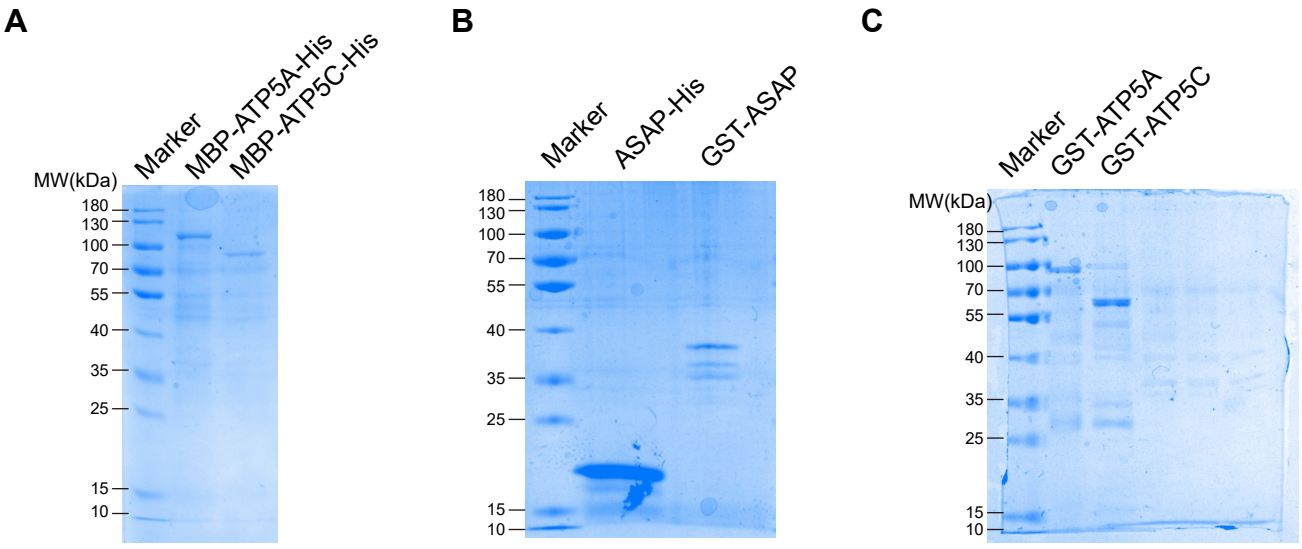
A
Marker
MBP-ATP5A-His
MBP-ATP5C-His
MW(kDa)
180
130
100
70
55
40
35
25
15
10
B
Marker
ASAP-His
GST-ASAP
180
130
100
70
55
40
35
25
15
10
C
Marker
GST-ATP5A
GST-ATP5C
MW(kDa)
180
130
100
70
55
40
35
25
15
10

Figure S15

Table S2. Genomic locations of 5 predicted ORFs of LINC00467.

ORF	Start	Stop	Length (aa)
1	196	480	94
2	230	322	30
3	338	550	70
4	650	796	49
5	453	596	47

Table S4. The sequence of siRNAs, gRNAs, donor oligos and primers used in the study.

The sequence of siRNAs:

Gene name	Sequence (5'-3')
LINC00467	si#1: GCUCUGUAAACCACAUAAUUU
	si#2: GGGAUUUGAAUUUGAACAUUU

The sequence of gRNAs and donor oligos:

FLAG knocking in in cell line	
gRNA	ATATGTTTTCTTTTGTTTTAAGG
Donor oligos	TTTATTGAAGCAATCATTAATATGTTTTCTTTTGTTTTAAGGACAAAATAGAT TACAAGGACGACGATGACAAGTGAAACACCAAGAAAAAGAGAAGGAAAAA AAGGAGGAAACAACCACATATGTC
ASRPS knocking out in cell line	
gRNA	GCAGGGAGGTTTAATAGACATGG
Donor oligos	AATGTGTCAATATTTTGGTTTTATAGACATGGCAGGGAGGTTTAATAGACAT TGATAAGAAGTCCACTCACAGAAATCCTGAAGATGCCAGGGCTGGCAAATA
ASRPS knocking out in PDX model	
gRNA	ACAGAAATCCTGAAGATGCCAGG

Primers used for RT-qPCR:

Gene name	Sequence (5'-3')
U6	Forward: CTCGCTTCGGCAGCACA
	Reverse: AACGCTTCACGAATTTGCGT
B2M	Forward: GGCTATCCAGCGTACTCCAA
	Reverse: TGGATGAAACCCAGACACATA
LINC00467	Forward: TTTCCAACATGGCAGGGAGG
	Reverse: GCCCTGGCATCTTCAGGATT
CRNDE	Forward: TATTCAGCCGTTGGTCTTTG
	Reverse: TCTGCGTGACAACTGAGGATT
SNHG17	Forward: TTTTCCCACGCTGTCTGTCA
	Reverse: CAGTTTCCCCCGATGGTGAG
ATP5A	Forward: CTCGCTTCGTTGCCACTTC
	Reverse: TAGGCGGCTCTATCTCTCGT
ATP5C	Forward: GGCTGTGGCTACCATGTTCT
	Reverse: GTCTCCTGGTGACATTGCGG

Table S5. Clinical correlation between ASAP expression and clinicopathological characteristics in colorectal cancer.

Clinicopathological Characters	Tumor ASAP Expression		χ^2	*p* Value (Chi-square test)
	High level (55)	Low level (37)		
Age (year)				
＜60	19	11	0.23	0.63
≥60	36	26		
Gender				
Male	26	17	0.02	0.90
Female	29	20		
Tumor Size (cm)				
＜5.0	19	34	29.78	0.00
≥5.0	36	3		
Invasive Depth				
T1 - T2	0	4	6.21	0.01
T3 - T4	55	33		
Lymph Node Metastasis				
N = 0	20	23	5.91	0.02
N = 1, 2, 3	35	14		
Distal Metastasis				
M = 0	32	25	0.83	0.36
M = 1	23	12		
TNM Stage (AJCC)				
Ⅰ - Ⅱ	15	17	3.40	0.06
Ⅲ - Ⅳ	40	20		